Knowledge-based Engineering and Sciences (2022), **3**, (1), 37–44
doi:10.51526/kbes.2022.3.1.37-44

RESEARCH PAPER

Numerical Simulation on the Effect of Pipe Roughness in Turbulent Flow

Mohammed Suleman Aldlemy,*[1,2] Sumaiya Jarin Ahammed,[3] Edgar Darío Obando,[4,5] and Maryam Bayatvarkeshi[6]

[1]Department of Mechanical Engineering, College of Mechanical Engineering Technology, Benghazi 11199, 9 Libya
[2]Center for Solar Energy Research and Studies (CSERS), Benghazi, Libya
[3]Department of Civil Engineering, International University of Business Agriculture and Technology, Dhaka 1230, Bangladesh
[4]National University of Colombia, E3P research group. Manizales, Caldas, Colombia
[5]Eslinga research group. Cooperative University of Colombia. Pasto-Colombia
[6]Geography and Environmental Management, University of Waterloo, Canada
*Corresponding author. Email: maldlemy@ceb.edu.ly

(Received 7 April 2022; revised 23 April 2022; accepted 26 April 2022; first published online 30 April 2022)

Abstract

Numerical simulations were performed to study the influences of pipe roughness and smoothness. 3D modeling was solved via ANSYS-Fluent v2021R1 under the condition of fully-developed turbulent flow in the range of $5{,}000 \leq \mathrm{Re} \leq 15{,}000$. The working fluid was distilled water, and thermal-physical properties were at 300K. The model $(k-\epsilon)$ was applied in the current study to solve the roughness problem with standard wall functions as the near-wall treatment. In the rough and smooth pipes, the pressure dropped by increasing the Reynolds number (Re). Meanwhile, the rough pipe showed higher pressure loss than a smooth pipe with an average of 40.34%. Moreover, the velocity contours were presented for both cases to discuss the effect of the rough wall on the velocity profiles.

Keywords: Turbulent flow; rough pipe; smooth pipe; pressure drop; velocity profiles

Nomenclatures

μ	Viscosity, Pa×s	μ	Viscosity, Pa×s
CFD	Computational Fluid Dynamics	D_h	Hydraulic Diameter, m
DW	Distilled Water	FVM	Finite Volume Method
k	Turbulence kinetic energy, $m^2 \times s$	k	Thermal conductivity, $W/m-K$
NIST	National Institute of Standards and Technology	P_{in}	Inlet pressure, Pa
P_{out}	Outlet temperature, Pa	Re	Reynolds number, $\left(R = \frac{\rho V_{in} D_h}{\mu}\right)$
T_{in}	Inlet temperature; K	V_{in}	velocity, m/s
ΔP	Pressure drop, Pa	ϵ	Turbulent dissipation rate, m^2/s^2
ρ	Density, kg/m^3		

1. Introduction

1.1 Research Background and Motivation

Turbulent flow over rough surfaces has become a hot topic in fluid dynamics and heat transfer [10]. This type of flow can be seen in heat exchangers, nuclear reactors, turbine blades, wind tunnels, fluid catalytic cracking, and airfoil, among other engineering applications [6], [16]. The effects of relative roughness and Reynolds number on velocity distribution and friction factor were investigated in pipe flow [7]. According to the findings, the relationship between velocity distribution and resistance formula could be extended from smooth pipes to rough pipes [19], [17]. Many experiments have been carried out to learn more about velocity distribution, pressure drop, and turbulent flow behaviour near rough walls [22, 13, 5, 14]] The heat transport as a function of roughness height to hydraulic diameter, spacing between Reynolds numbers, and roughness elements has been investigated in several research [21, 20, 4, 11].

1.2 Adopted Literature Review on the Roughness of Pipe in Turbulent Flow

The turbulence profile in all coordinate directions is determined by inspecting fluctuating velocity spectra in rough pipes. According to this research, the nature of the solid barrier has a negligible effect on the flow in the centre part of the pipe. The flow along the wall, on the other hand, is determined by the nature of the solid boundary. Several academics have offered alternative techniques to studying the link between turbulent flow and rough surfaces in the literature. The behavior of turbulent flow in ducts is investigated by using a roughness element drag coefficient [11]. Recently, a formula for calculating mean velocity over the inner layer of a turbulent boundary has been proposed. The friction factor correlation for the fully developed turbulent pipe flow is formulated using the velocity profile obtained by busing this formula [15]. Other significant works involving the application of the $(k-\epsilon)$ turbulence model were investigated [8]. The modified mixed length model provided a new technique for studying the rough wall's influence [23]. They also proposed a solution for pipe flow fields, both external and internal. When compared to other ways, this strategy has the advantage of being less expensive to compute. With moderate roughness and an acceptable degree of accuracy, the $(k-\epsilon)$ model can be utilized. The researchers concluded that the $(k-\epsilon)$ model with enhanced wall treatment among different turbulence models gives the most suitable prediction [3, 9].

1.3 Research Objectives

The present study deals with the CFD analysis of fully developed turbulent flow in a 3D pipe using $(k-\epsilon)$ turbulence model with enhanced wall treatment. Moreover, the turbulent flow in the range of $5{,}000 \leq \mathrm{Re} \leq 15{,}000$ and the thermal-physical properties were under 300K as inlet temperature. Two pipes were tested such as rough and smooth, to discuss the effect of roughness on the value of pressure drop and the model. The contours of wall function are also shown to see the effect of enhanced wall treatment.

2. Numerical Parameters and Procedures

2.1 Physical Model and Assumptions

Increasing the pressure drop of the working fluid along a circular rough and smooth pipe was numerically solved using CFD under fully-developed turbulent flows. The pipe cross-section of the horizontal circular pipe was presented in Figure 1. The total pipe length is 500 mm, the diameter is 20 mm. A grid was created using the meshing module of ANSYS-Fluent v2021R1. The physical domain modeled the fluid control volume and did not account for the tube wall thickness. Figure 1 presents the computational domain. Its 15 inflation layers were used to mesh the region adjacent to the walls, which were used to mesh the region adjacent to the walls due to significant velocity and temperature gradients.

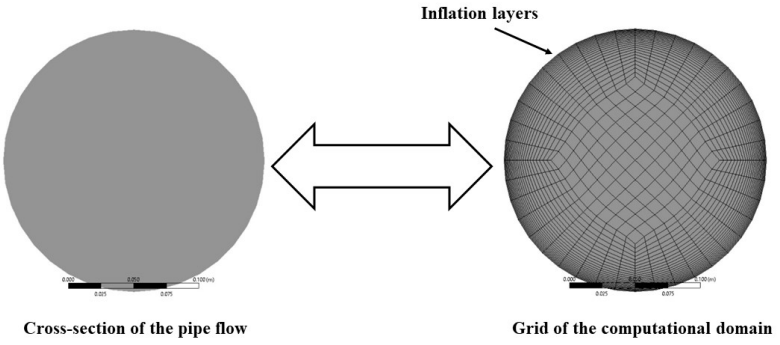

Figure 1: *(left) Cross-section of the pipe flow, and (right) grid of the computational domain.*

2.2 Governing Equations

The conservation of mass, momentum for the efficient model are as follows [18, 2]

$$\nabla \rho \bar{V} = 0, \tag{1}$$

$$\nabla \rho \bar{V} \bar{V} = -\nabla \bar{P} + \mu \nabla^2 \bar{V} - \rho \nabla \overline{v v}, \tag{2}$$

where $\bar{V}$ and $\bar{P}$ are the time-averaged flow variables, while $\bar{v}$ is the velocity fluctuation(s). The momentum equation $\rho \nabla \overline{v v}$ represents the turbulent shear stress.

The two equations model is the most famous and straightforward turbulence model. In this model the length scales and turbulent velocity are calculated independently by using the solution of different transport equations. The standard $(k - \epsilon)$ model has become the widely used turbulence model for the solution of practical engineering flow problems by Launder and Spalding [12]. Such a semi-empirical model is built on transport equations for the turbulence kinetic energy (k) and its dissipation rate (ϵ). The model transport equation for (k) is derived from the exact equation, while the model transport equation for (ϵ) was obtained using physical reasoning and bears little resemblance to its mathematically precise counterpart.

$$\nabla(\rho k V) = \nabla \left[\left(\frac{\mu_t}{\sigma_k} \right) \nabla k \right] + G_k - \rho \epsilon \tag{3}$$

$$\nabla(\rho \epsilon V) = \nabla \left[\left(\frac{\mu_t}{\sigma_k} \right) \nabla k \right] \frac{\epsilon}{k} (C_{1\epsilon} G_k - C_{2\epsilon} \rho \epsilon) \tag{4}$$

$$G_k = \mu_t (\nabla V + (\nabla V)^\top), \quad \mu_t = \rho C_u \frac{k^2}{\epsilon} \tag{5}$$

$$C_u = 0.09, \quad \sigma_k = 1, \quad \sigma_\epsilon = 1.3, \quad C_{1\epsilon} = 1.44, \quad C_{2\epsilon} = 1.92 \tag{6}$$

In this regard, μ is the effective viscosity of working fluid, while μ_t is the viscosity coefficient in a turbulent regime.

The boundary conditions (BCs) are outlined in this section for solving the CFD model's governing equations. The pipes' walls were smooth and rough, and its external surface was insulated. The working fluids enter the pipe at a constant inlet temperature (T_{in} = 300K), with a uniform axial velocity (V_{in}). The finite volume method (FVM) was used to discretize partial differential equations

(Governing equations) into linear algebraic equations, making them numerically solvable. The second-order upwind scheme was used to discretize the convection and diffusion terms, and other appropriate variables appear in the governing equations. The velocity components are evaluated at the center of the control volume interfaces in staggered grid designs. All scalar quantities are estimated at the control volume's center. The Semi Implicit Method for Pressure Linked Equations [SIMPLE] was used to link pressure and velocity. ANSYS CFD uses a point implicit (Least Squares Cell Based) linear equation solver and an algebraic multigrid approach to solve the linear systems produced from the discretization schemes. The residuals monitors were convergence with an absolute criterion of $< 10^{-6}$.

2.3 Validation and Verification of Simulations

Four different computational domains are tested for grid independence test, such as 90,277, 109,863, 161,850, and 222,222 elements, See Table 1. The second grid (109,863 elements) is adopted in the next simulations due to it's very less error with the previous grid with 0.59%. Meanwhile, the third and fourth grids show an error of 5.22% and 9.96%, respectively. The current model was validated with the data of A.H. Abdelrazek et al. [1]. The pressure drop values show a good agreement with an average error of 8.5%, as shown in Fig 2.

Table 1: *Grid independence test at Re = 5,000.*

Mesh	Elements	P_{in}	P_{out}	∇P	Error
1	90,277	31.69884	4.902894	26.79594	-
2	109,863	31.71926	4.762929	26.95633	0.59%
3	161,850	31.75175	3.31054	28.44121	5.22%
4	222,222	31.80573	0.219329	31.5864	9.96%

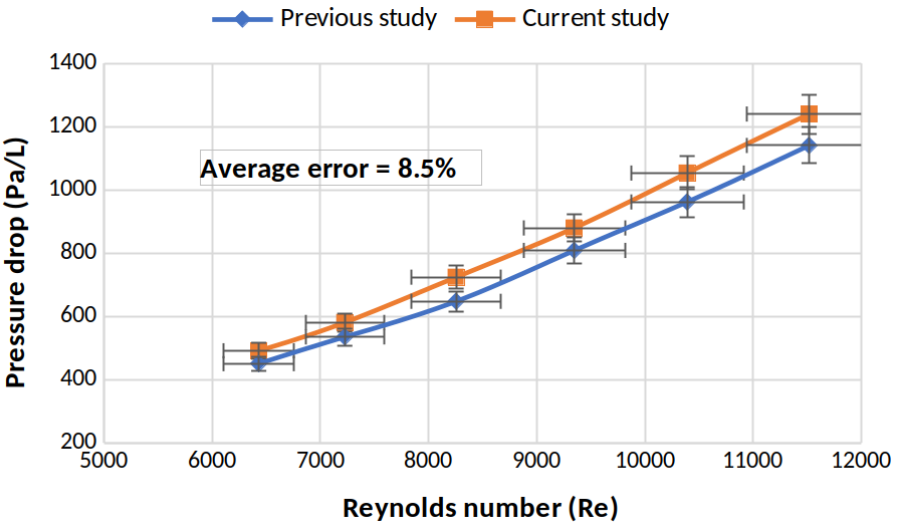

Figure 2: *Comparison between the current model and A.H. Abdelrazek et al. [1].*

3. Results and Discussion

Evaluation of pressure drop, and flow features should be deeply considered side by side with the heat transfer measurements for different working fluids as long as they are used for practical purposes. Fig. 3 shows the pressure loss of rough and smooth pipes versus the Reynolds number of the circular modelling. As can be seen, the pressure loss increases with the increase of Reynolds number for both cases due to the increment in the fluid velocity along the pipe. As expected, the pressure dropped higher in the rough pipe more than the smooth pipe, with an average increment of 40.43%. The rough and smooth pipe show almost the same values of inlet pressure; meanwhile the values of outlet pressure of rough pipe are lower than the smooth pipe. The current results show s clear evidence that the smooth pipe is preferable in thermal and engineering applications because it's moderate pressure loss. As we know, the higher-pressure loss will consume more pumping power, which is considered uneconomic.

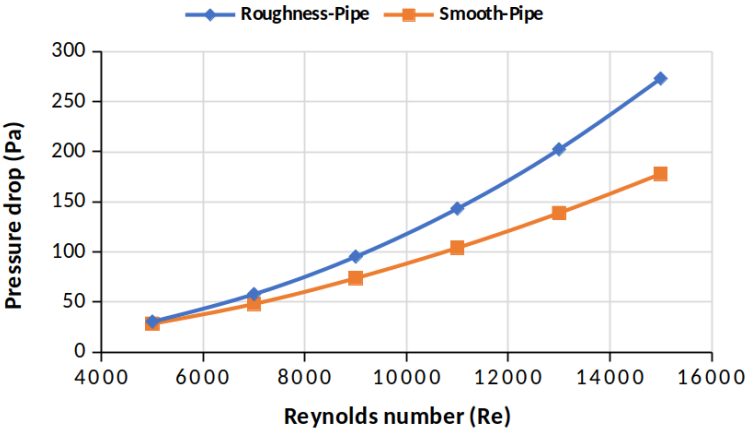

Figure 3: *Pressure drop data of rough and smooth pipes versus Reynolds number.*

The contours of velocity profiles are presented in Fig. 4 and Fig. 5 for the rough and smooth pipes versus the Reynolds number. It can be seen from Fig. 4 and Fig. 5 that, the outlet velocity of the smooth pipe shows higher values than the rough pipe. The outlet pressure of smooth pipe is always higher than the outlet pressure of rough pipe due to the value of outlet velocity. In contrast, the parameter (p_{in}-P_{out}) of rough pipe is higher and influenced by higher pumping power.

4. Conclusions

The influences of pipe roughness and smoothness were discussed numerically. The working fluid was distilled water, and thermal-physical properties were at 300K. The model ($k-\epsilon$) was applied in the current study in the range of 5,000 $\leq$ Re $\leq$ 15,000. The followings conclusions could be drawn:

1- The thermal-physical properties of distilled water at 300K were collected from the National Institute of Standards and Technology (NIST) database.
2- The pressure dropped with the Reynolds number (inlet velocity) increase for both cases (rough and smooth).
3- The roughness of pipe showed a significant impact on the values of pressure drop more than smooth pipe.
4- Velocity profiles (contours) illustrated the boundary layers of both pipes and explained the real reason for higher-pressure loss in rough pipes.

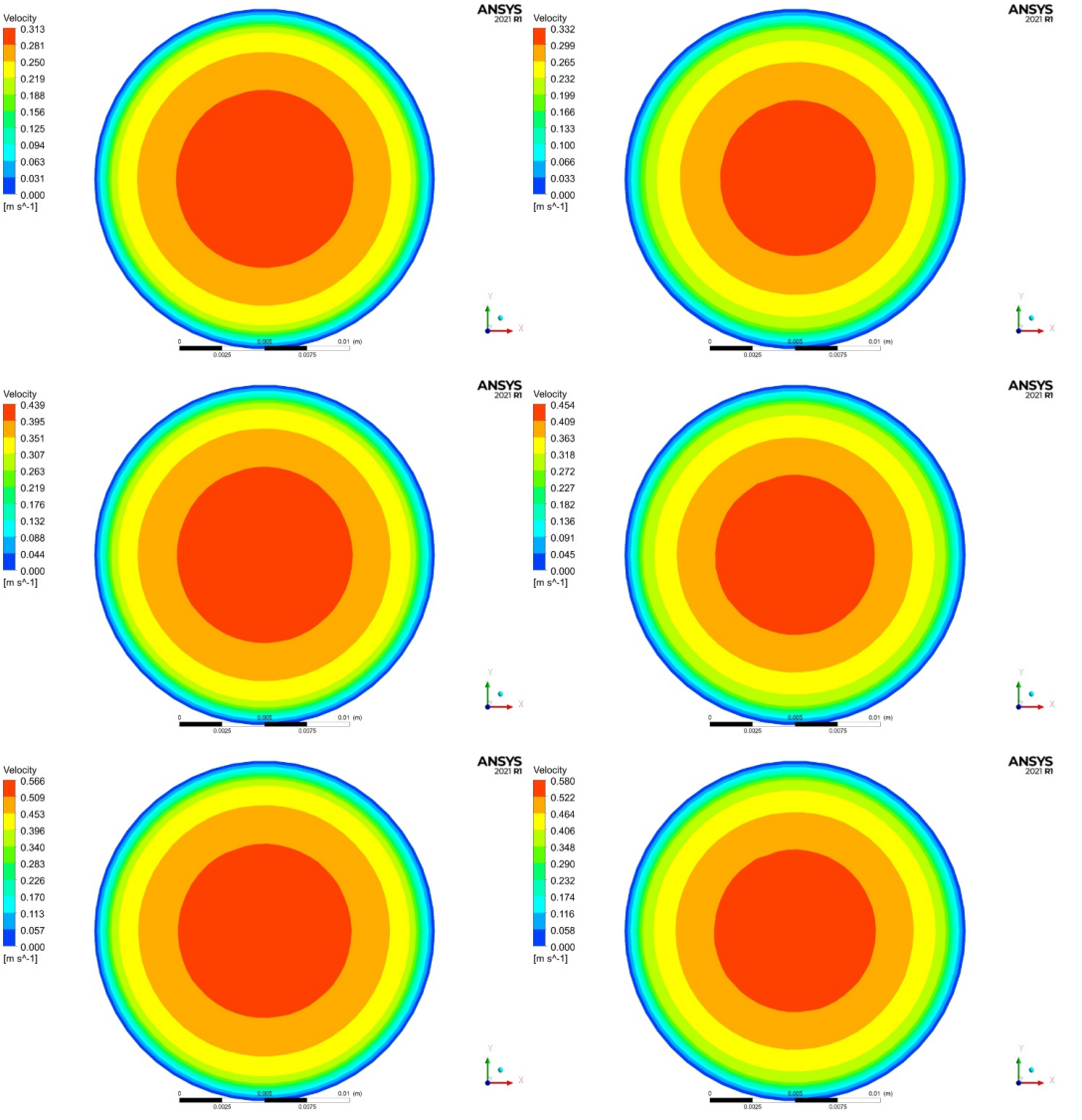

Figure 4: *Contours of velocity profiles at the outlet of rough and smooth pipes versus Reynolds number.*

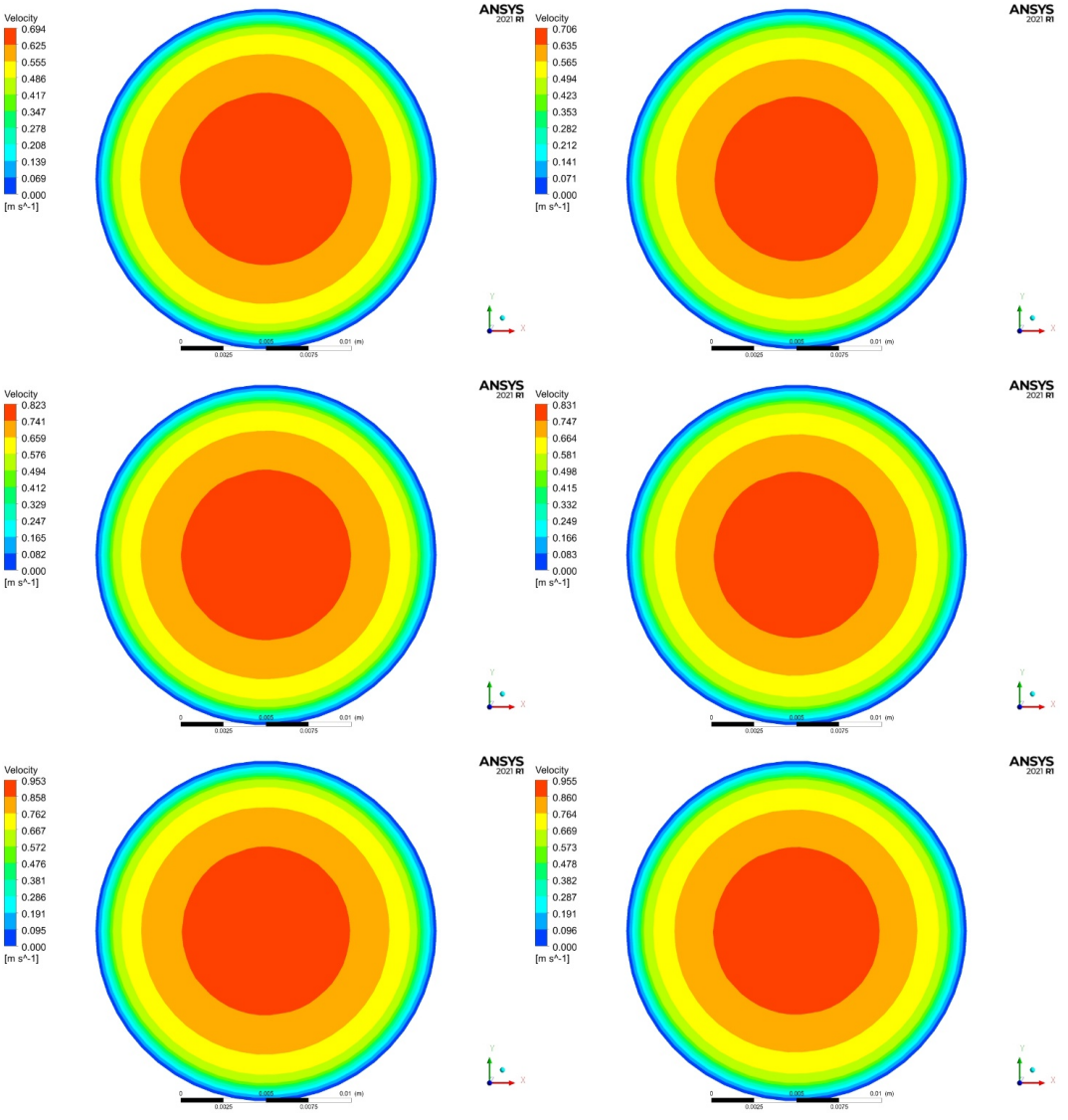

Figure 5: *Contours of velocity profiles at the outlet of rough and smooth pipes versus Reynolds number.*

Conflicts of Interest: **The authors have no conflict of interest to any part.**

References

[1] A. H. Abdelrazek et al. "A new approach to evaluate the impact of thermophysical properties of nanofluids on heat transfer and pressure drop". In: *Int. Commun. Heat Mass Transf.* 95 (2018), pp. 161–170.

[2] A. H. Abdelrazek et al. "Heat transfer and pressure drop investigation through pipe with different shapes using different types of nanofluids". In: *J. Therm. Anal. Calorim.* 139 (2020), pp. 1637–1653.

[3] M. Ahsan. "Numerical analysis of friction factor for a fully developed turbulent flow using k-ϵ turbulence model with enhanced wall treatment". In: *Beni-Suef Univ. J. Basic Appl. Sci.* 3.4 (2014), pp. 267–277.

[4] O. A. Alawi et al. "Effects of binary hybrid nanofluid on heat transfer and fluid flow in a triangular-corrugated channel: An experimental and numerical study". In: *Powder Technol.* 395 (2022), pp. 267–279.

[5] O. A. Alawi et al. "Heat transfer and hydrodynamic properties using different metal-oxide nanostructures in horizontal concentric annular tube: An optimization study". In: *Nanomaterials* 11.8 (2021), p. 1979.

[6] A. M. Aly and G. Bitsuamlak. "Aerodynamics of ground-mounted solar panels: test model scale effects". In: *J. Wind Eng. Ind. Aerodyn* 123 (2013), pp. 250–260.

[7] P. Bradshaw. "A note on critical roughness height and transitional roughness," in: *Phys. Fluids* 12.6 (2000), pp. 1611–1614.

[8] N. D. Cardwell, P. P. Vlachos, and K. A. Thole. "Developing and fully developed turbulent flow in ribbed channels". In: *Exp. Fluids* 50.5 (2011), pp. 1357–1371.

[9] K. A. Hafez, O. A. Elsamni, and K. Y. Zakaria. "Numerical investigation of the fully developed turbulent flow over a moving wavy wall using k-ϵ turbulence model". In: *Alexandria Eng. J.* 50.2 (2011), pp. 145–162.

[10] M. Kadivar, D. Tormey, and G. McGranaghan. "A review on turbulent flow over rough surfaces: Fundamentals and theories". In: *Int. J. Thermofluid* 10 (2021), p. 100077.

[11] S. G. Kandlikar et al. "Characterization of surface roughness effects on pressure drop in single-phase flow in minichannels". In: *Phys. Fluids* 17.10 (2005), p. 100606.

[12] B. E. Launder and D. B. Spalding. "The numerical computation of turbulent flows". In: *Comput. Methods Appl. Mech. Eng.* 3.2 (1974), pp. 269–289.

[13] S. Liu et al. "Energy analysis using carbon and metallic oxides-based nanomaterials inside a solar collector". In: *Energy Rep.* 6 (2020), pp. 1373–1381.

[14] R. S. Mohammad et al. "Solar radiation forecasting in Nigeria based on hybrid PSO-ANFIS and WT-ANFIS approach". In: *Nanomaterials* 11.11 (2021), p. 3094.

[15] C. Di Nucci and A. R. Spena. "Mean velocity profiles of two-dimensional fully developed turbulent flows". In: *Comptes Rendus Mecanique* 340.9 (2012), pp. 629–640.

[16] L. C. G. Pimentel, R. M. Cotta, and S. Kakac. "Fully developed turbulent flow in ducts with symmetric and asymmetric rough walls". In: *Chem. Eng. J.* 74.3 (1999), pp. 147–153.

[17] M. R. Rasani, M. S. Aldlemy, and Z. Harun. "Fluid-structure interaction analysis of rear spoiler vibration for energy harvesting potential". In: *J. Mech. Eng. Sci.* 11.1 (2017), pp. 2415–2427.

[18] R. Sadri et al. "CFD modeling of turbulent convection heat transfer of nanofluids containing green functionalized graphene nanoplatelets flowing in a horizontal tube: Comparison with experimental data". In: *J. Mol. Liq.* 269 (2018), pp. 152–159.

[19] G. Singh and O. D. Makinde. "Computational dynamics of MHD free convection flow along an inclined plate with Newtonian heating in the presence of volumetric heat generation". In: *Chem. Eng. Commun.* 199.9 (2012), pp. 1144–1154.

[20] A. O. Al-Sulttani et al. "Thermal effectiveness of solar collector using Graphene nanostructures suspended in ethylene glycol-water mixtures". In: *Energy Rep.* 8 (2022), pp. 1867–1882.

[21] H. Togun, S. N. Kazi, and A. Badarudin. "A review of experimental study of turbulent heat transfer in separated flow". In: *Aust. J. Basic Appl. Sci.* 5.10 (2011), pp. 489–505.

[22] S. Vijiapurapu and J. Cui. "Performance of turbulence models for flows through rough pipes". In: *Appl. Math. Model.* 34.6 (2010), pp. 1458–1466.

[23] J. Zhu and A. V Kuznetsov. "Forced convection in a composite parallel plate channel: modeling the effect of interface roughness and turbulence utilizing ak-ϵ model". In: *Int. Commun. heat mass Transf.* 32.1-2 (2005), pp. 10–18.